Cell Reports
Physical Science

Article

Strain-release photocatalytic access to rigidified isosteres of bicyclic heterocycles

Graphical abstract

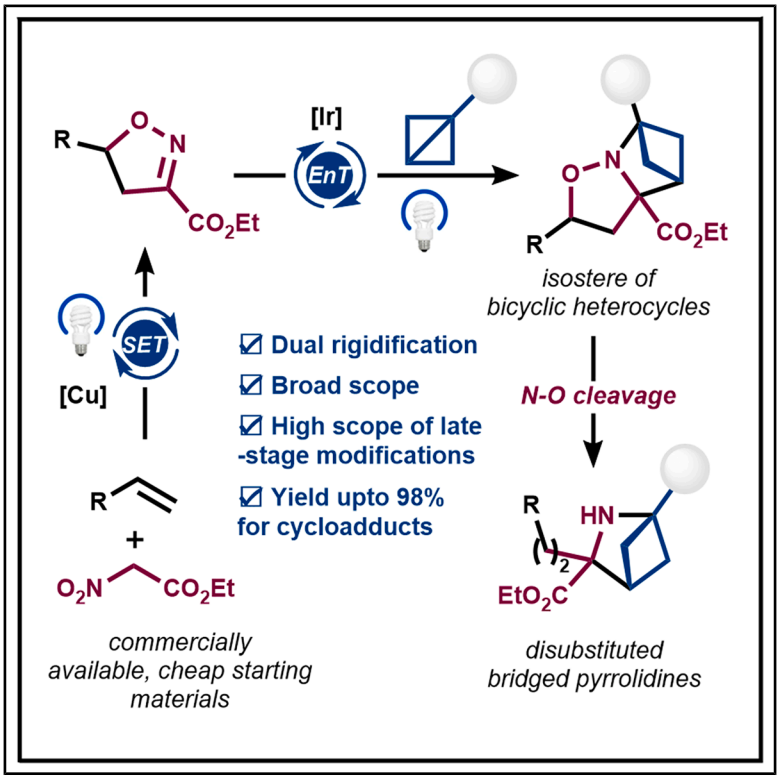

Authors

Sunaina Sardana, Oliver Reiser

Correspondence

oliver.reiser@chemie.uni-regensburg.de

In brief

Sardana et al. report the synthesis of bridged pyrrolidines and proline derivatives in an overall two-step, light-driven sequence with high atom economy. In this way, sp^3- and heteroatom-rich isosteres relevant to medicinal chemistry are obtained.

Highlights

- Synthesis of rigid carbocycles by photocycloaddition of isoxazolines and bicyclobutanes
- Dual-rigidification achieved by fusion and bridging
- Single-step modification of the products gives access to substituted bridged pyrrolidines
- Linear light-driven synthesis: key reactant isoxazolines are also made via photocatalysis

Sardana & Reiser, 2026, Cell Reports Physical Science 7, 103449
August 19, 2026
https://doi.org/10.1016/j.xcrp.2026.103449

CellPress

Cell Reports
Physical Science

CellPress
OPEN ACCESS

Article

Strain-release photocatalytic access to rigidified isosteres of bicyclic heterocycles

Sunaina Sardana[1] and Oliver Reiser[1,2,*]
[1]Department of Organic Chemistry, University of Regensburg, Universitätsstr. 31, 93053 Regensburg, Germany
[2]Lead contact
*Correspondence: oliver.reiser@chemie.uni-regensburg.de
https://doi.org/10.1016/j.xcrp.2026.103449

SUMMARY

We present the synthesis of fused isoxazolidine-pyrrolidine architectures via a dual rigidification strategy. These frameworks are accessed through an atom-economical approach using variously substituted isoxazolines and bicyclo[1.1.0]butane (BCB) derivatives under mild conditions. Subsequent functionalization of these analogs enables the synthesis of structurally diverse, disubstituted bridged pyrrolidines and proline derivatives that are otherwise challenging to access. This approach efficiently generates complex, rigid scaffolds, thereby expanding the chemical space available for the design of medicinally relevant small molecules.

INTRODUCTION

The benzene ring and other heterocycles serve as a fundamental scaffold in medicinal chemistry.[1–6] However, the presence of flat aromatic rings in the cores of drug molecules often contributes to their poor aqueous solubility and metabolic stability.[7–11] Hence, numerous strategies have been proposed to replace or modify such structures to "escape from flatland."[12–14]

One approach involves substituting the benzenoid core with a saturated ring such as cyclohexane, which can enhance metabolic stability and reduce off-target interactions.

However, such substitution leads to the loss of conformational rigidity, a crucial characteristic that enables molecules to exhibit desirable pharmacological properties. Thus, the challenge is 2-fold, i.e., increasing the proportion of saturated carbon atoms while mimicking the steric properties characteristic of an aromatic ring (isosteres). Although aromatic bicyclic cores are common in drugs such as bufuralol and zolpidem, the increasing use of saturated rigid analogs such as gliclazide and some HIV inhibitors highlights the need for new synthetic approaches.

Rigidification of saturated rings can be achieved by bridging, which has been proposed as a replacement for substituted phenyl cores[15–18] (Figure 1A). Modern synthetic strategies have been utilized fruitfully to develop bioisosteres of substituted benzenes[16] and pyridines.[19] 3D enhancement of another key molecule in medicinal chemistry, pyrrolidines, has also been proposed.[12,20] Moieties containing 2,4-methanopyrrolidines (a bridged pyrrolidine structure) have shown superior physiological properties compared to simple pyrrolidines.[21] Hence, cost-effective synthetic routes to access such bridged cores are desirable. Another popular tactic to restrict conformational flexibility is the fusion of two carbocycles,[22,23] which was elegantly demonstrated by Mykhailiuk and co-workers for accessing bioactive fused-pyrrolidines.[24–26] The hunt for synthetic routes to obtain rigidified structural motifs has taken a new direction with the increasing use of bicyclo[1.1.0]butanes (BCBs) as a versatile moiety owing to their strained C–C σ bond that is amenable to a plethora of transformations under different conditions, including photocatalytic electron transfer, energy transfer (EnT), and thermal pathways.[27–49]

Among them, $[2_\pi+2_\sigma]$ cycloadditions mediated by EnT under mild conditions have been disclosed by Glorius,[29,30,33,34] Brown,[31,45,47] and Waser,[44] among others.[50] Furthermore, Lewis acid-mediated coupling reaction of BCBs with moieties such as ketenes,[51] aldehydes,[52] dienol ethers,[44] ynamides,[53] and imidazoles[54] have also been reported as effective methods for accessing structurally complex saturated frameworks.[55,56] Among these, the cycloaddition of imines on BCBs carries special importance because it gives one-step access to bridged pyrrolidines, and this has been achieved by Guo,[40] Leitch,[57] Zhou,[58] Feng,[59] Lu,[60] and Li[61] and co-workers. Although the synthesis of isostere of monocyclic and tricyclic systems has been extensively investigated, those for bicyclic heterocycles remain largely underexplored, with only a few examples reported by Glorius and co-workers through dearomative cycloadditions with BCBs.[29,41]

In this study, we report a broadly applicable, one-step photocatalytic methodology to afford sp^3-rich bicyclic and tricyclic frameworks via the $[2_\pi+2_\sigma]$ cycloaddition between cyclic oximes and BCBs. To the best of our knowledge, only a single example of such a cycloaddition was reported under near-UV irradiation (λ_{max} = 405 nm) using thioxanthone (TXT) as the photocatalyst.[34] The structural motif, a "fusion" of isoxazolidine and a "bridged" pyrrolidine, provides a dually rigidified core with a high potential to serve as an isostere of bicyclic cores (Figure 2B).[23,62–66]

RESULTS AND DISCUSSION

Reaction development

We initiated our investigation by selecting readily prepared isoxazoline[67] **1a** for the desired coupling with BCB-morpholine **2a**.

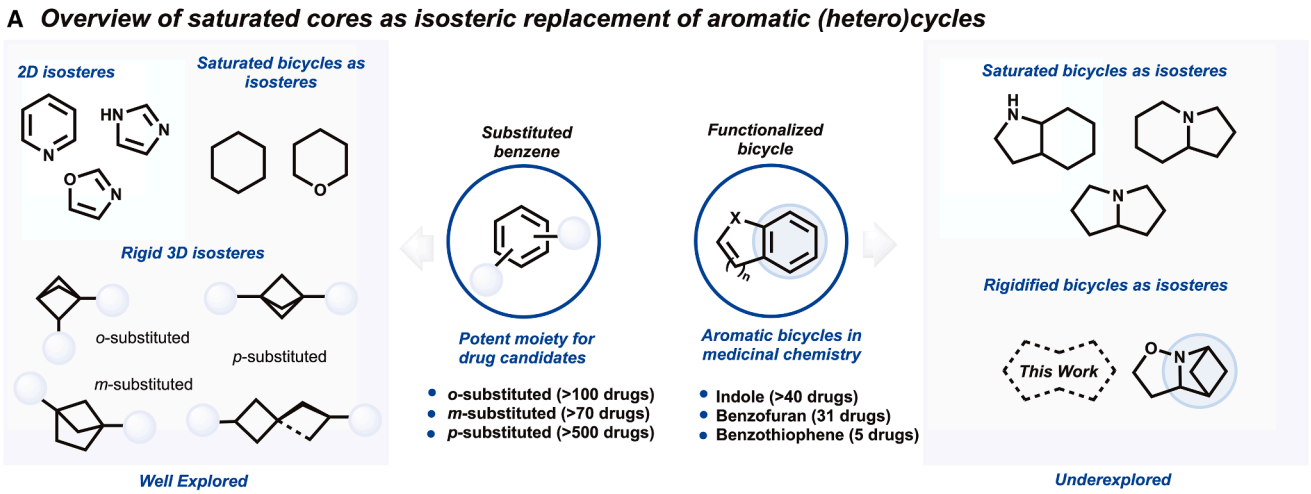

Figure 1. Structures relevant for this study

(A) Isosteres of aromatic (hetero)cycles.

(B) Drugs containing fused heterocycles.

Initial experiments evaluated various photocatalysts, revealing that $Ir(dFppy)_3$ (1 mol %) exhibited superior catalytic activity that afforded **3a** in 98% yield (Table 1). The catalyst loading could be further reduced to 0.5 mol % without loss in reaction efficiency (entry 2). Furthermore, the Ir-F complex delivered the desired product in 96% yield (entry 3). Related

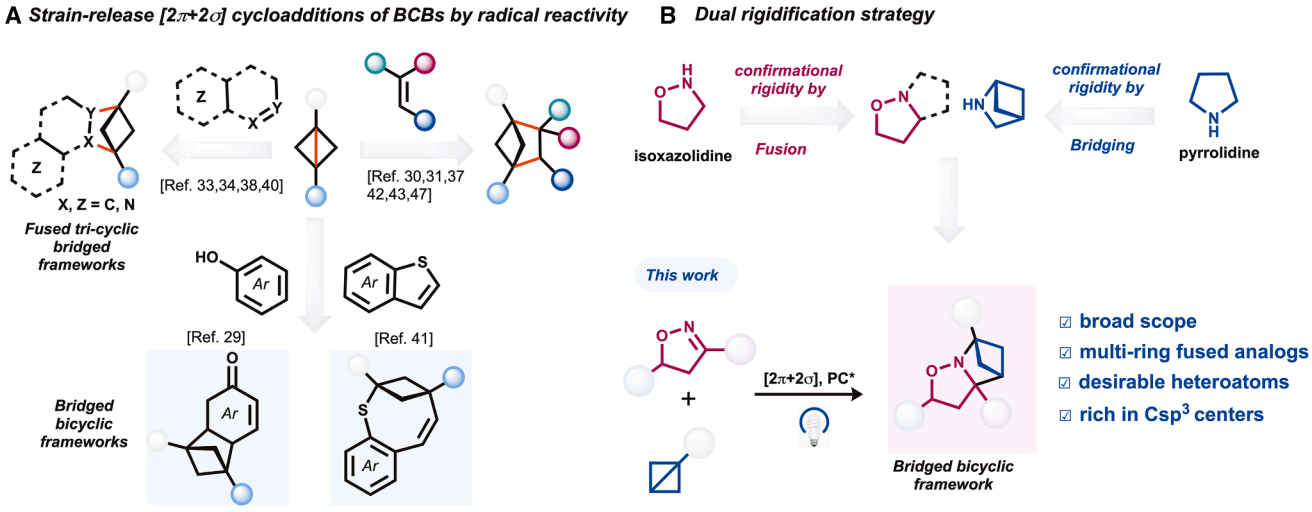

Figure 2. State of the art

(A) Reported cycloadditions of BCBs.

(B) Overview of dual rigidification strategy and this work.

Table 1. Optimization of the reaction conditions

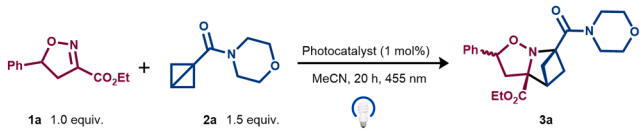

Entry[a]	Variation	Yield[b]
1	Ir(dF)ppy$_3$	>98
2	Ir(dF)ppy$_3$ (0.5 mol %)	98
3	Ir-F	96
4	Ir(ppy)$_2$(dtbbpy)PF$_6$	64
5	Ir(ppy)$_3$	<10
6	4-CzIPN	39
7	Cu(phen)(xantphos)BF$_4$	22
8	1,4-dioxane	36
9	no PC	n.r.
10	no light	n.r.

Structure of Ir-Photocatalysts:

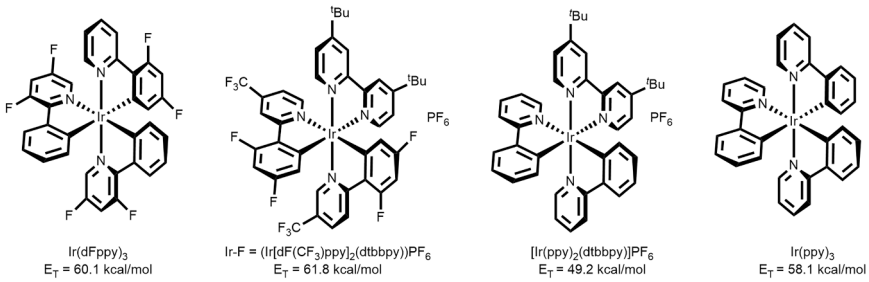

n.r., no reaction. E_T = triplet energy.
[a]Reaction conditions: isoxazoline **1a** (0.1 mmol, 1.0 equiv), BCB **2a** (0.15 mmol, 1.5 equiv), photocatalyst (10 μmol, 1.0 mol %) in solvent (1 mL, 0.1 M), and irradiation at 455 nm (6W) for 20 h at room temperature.
[b]^{1}H-NMR yield calculated using 1,1,2,2-tetrachloroethane as an internal standard.

Ir complexes also gave the desired product but in lower yields (entries 4 and 5). The use of other EnT photocatalysts, such as 4-CzIPN and Cu(phen)(xantphos)BF$_4$, afforded **3a** in significantly lower yields (entries 6 and 7). No product was observed for copper homoleptic complexes (see the supplemental methods for more details). Control experiments established that both light and the photocatalyst are indispensable for the reaction to proceed. Two diastereomers for **3a** were identified, differing in whether the phenyl group on the isoxazolidine ring is *cis* or *trans* to the ester substituent. The major diastereomer was determined by the 2D NMR spectrum of **3ah** to be the *trans*-isomer based on the Nuclear Overhauser Effect (NOE) correlation between the distinguishable benzylic proton and the aliphatic proton of the bicyclic fragment in both diastereomers (for details, see the supplemental methods).

With the optimized reaction conditions in hand, the general applicability of the title reaction was investigated (Figure 3). The scope of aryl-substituted isoxazolines **1a** was explored using BCB **2a**, affording the corresponding cycloadducts **3a**–**3i** in 89%–98% yield. Moreover, the reaction was successfully scaled up to 4 mmol, yielding **3a** in 88% (1.36 g). A 4-phenyl-substituted arene on the isoxazoline showed a better diastereomeric ratio of the major product **3f**. Inspired by the work of Zhong and co-workers,[68] the methodology was extended to fused carbocycle-bearing isoxazolines to access multi-ring saturated frameworks such as **3l** and **3m**. These fused architectures enrich the sp^3 content of the product motifs and incorporate significant rigidity into the molecule.

Likewise, isoxazolines with aliphatic substituents were found to be equally effective, affording the target products **3n**–**3r** in >90% yield. Moreover, ester functionalities on the C5 position were equally tolerated, yielding products **3s** and **3t** in very good yields.

To further improve the stereoselectivity, we explored naphthyl-substituted isoxazoline and successfully delivered the desired product **3u** in a moderate yield. The methodology was tolerant of isoxazolines derived from complex molecules, affording products **3v** and **3w**.

Next, emphasis was given to modulate the functional groups on the C3 position to explore the generality of the developed

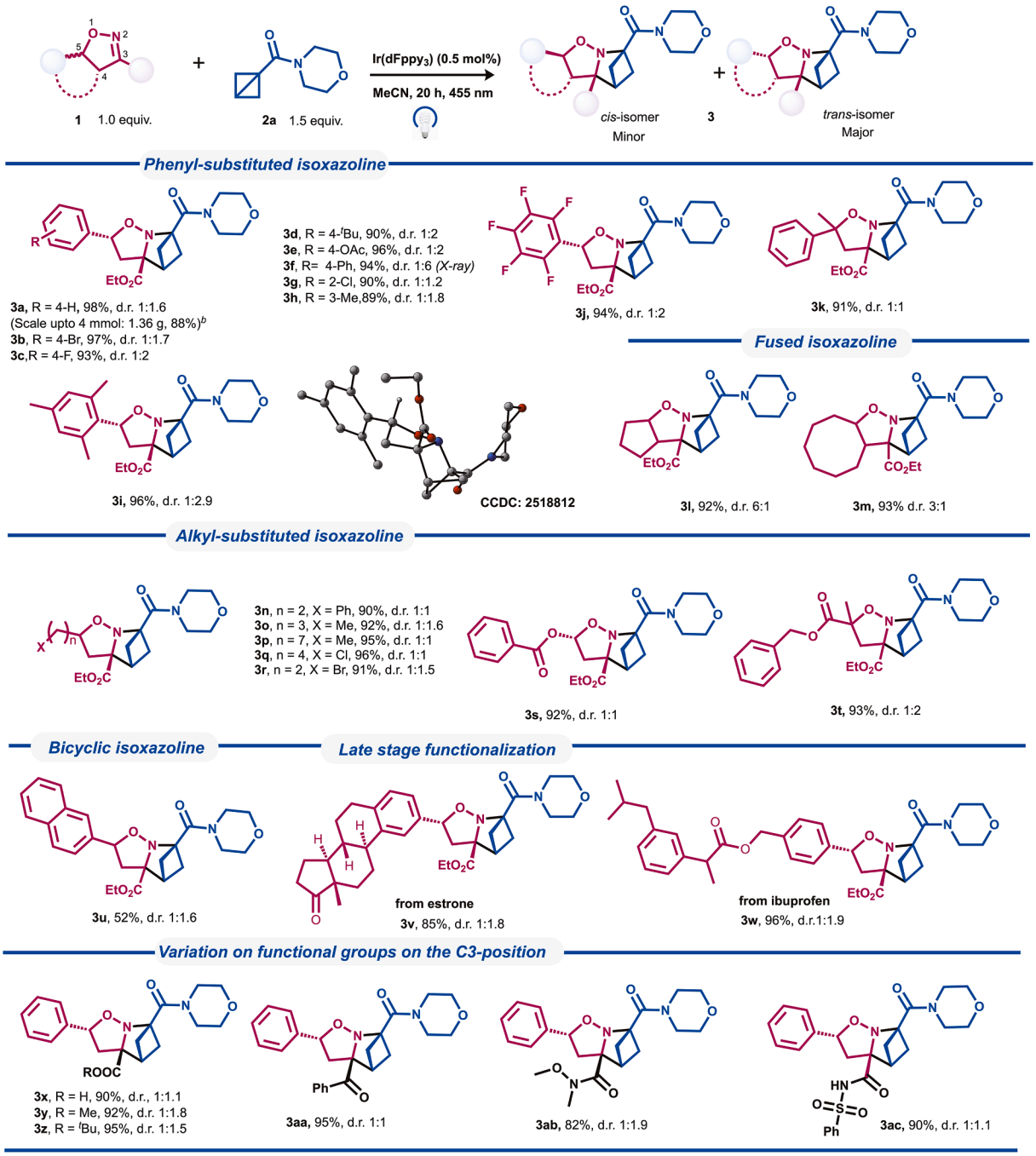

Figure 3. Scope isoxazolines

Reaction conditions: isoxazoline **1** (0.1 mmol, 1.0 equiv), BCB **2a** (0.15 mmol, 1.5 equiv), and $Ir(dFppy)_3$ (0.5 mol %) in MeCN (0.1 M) at room temperature under irradiation with blue LEDs (λ_{max} = 455 nm) for 20 h. Isolated yields are indicated.

[a]Diastereomeric ratio (dr) was determined by ^{1}H-NMR analysis of the crude reaction mixture.

[b]The reaction time was increased to 36 h.

method. To our delight, different functional groups such as acid, methyl ester, *tert*-butyl ester, ketone, Weinreb amide, and sulfonamide furnished the target products **3x**–**3ac** in good yields (82%–95%). These results indicate that the reactive site of the substrate, specifically the C–N π-bond, remains largely unperturbed by various substitutions on the isoxazoline core.

A series of BCB derivatives with diverse amide functionality was systematically tested with isoxazoline **1a** (Figure 4). Acyclic N,N-disubstituted BCB amides as well as cyclic amides

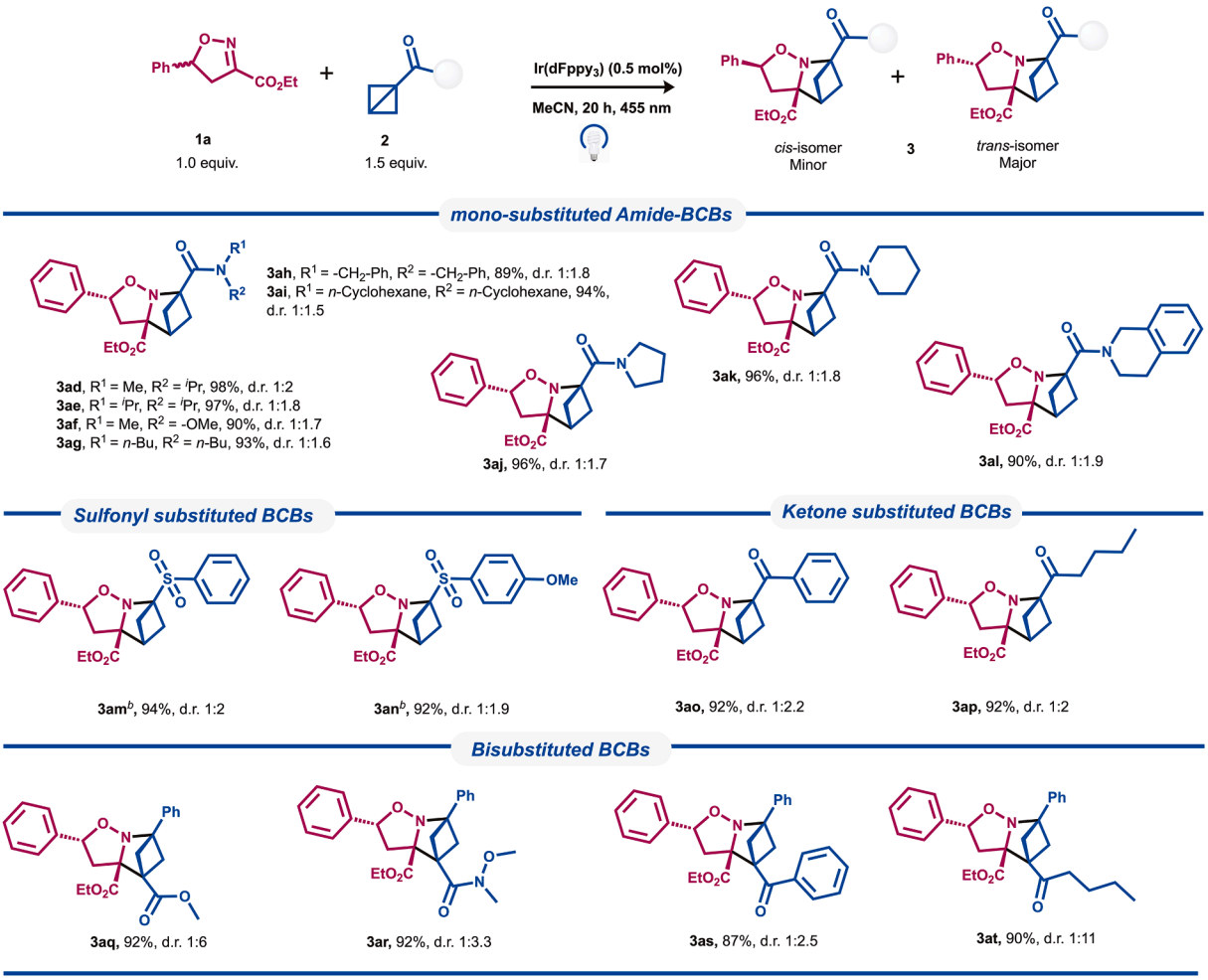

Figure 4. Scope BCBs

Reaction conditions: isoxazoline **1a** (0.1 mmol, 1.0 equiv), BCB **2** (0.15 mmol, 1.5 equiv), and Ir(dFppy)$_3$ (0.5 mol %) in MeCN (0.1 M) at room temperature under irradiation with blue LEDs (λ_{max} = 455 nm) for 20 h. Isolated yields are indicated.

[a]Diastereomeric ratio (dr) was determined by ^{1}H-NMR analysis of the crude reaction mixture.

[b]Reaction time was 30 h.

were smoothly converted to the desired products (**3ad–3al**). Also, sulfonyl- and ketone-substituted BCBs provided products **(3am–3ap)** in high yields. Furthermore, bisubstituted BCBs were also equally compatible, giving the target products (**3aq–3at**) in good yields.

Mechanistic studies

To elucidate the reaction mechanism, a series of experimental investigations was conducted along with density functional theory (DFT) calculations.

Cyclic voltammetry established that isoxazoline **1a** displays a high oxidation potential (E_{ox} = +2.36 V vs. saturated calomel electrode [SCE]) and a comparatively negative reduction potential (E_{red} = −1.34 V vs. SCE). These values lie well beyond the excited-state redox window of Ir(dFppy)$_3$ ($E_{ox}^{II/III*}$ = +0.36 V vs. SCE and $E_{red}^{III*/IV}$ = −1.28 V vs. SCE),[69] rendering both oxidative and reductive quenching pathways thermodynamically inaccessible. Consequently, direct single-electron transfer (SET) between **1a** and the excited photocatalyst can be excluded (Figure 5A).

Given the well-documented ability of iridium-based photocatalysts to mediate EnT processes with excitable cyclic oximes,[70] an EnT mechanism is proposed to govern the reaction pathway (Figure 6). Stern-Volmer luminescence quenching studies identified isoxazoline **1a** (Ksv = 0.165 mM^{-1}) as the primary quencher of the excited photocatalyst, while BCB **2a** (Ksv = 0.013 mM^{-1}) showed negligible quenching (Figure 5B).

The reaction profile was computed using the DFT method B3LYP-D3BJ/def2-TZVP with acetonitrile as implicit solvent included in the solvation model based on density (SMD model; Figure 7). The calculated triplet energies (E_T) for isoxazoline **1a** (55.9 kcal/mol) were found to be lower than those of BCB **2a** (78.6 kcal/mol), corroborating the quenching studies. Thus, the triplet energy from the excited photocatalyst is transferred to

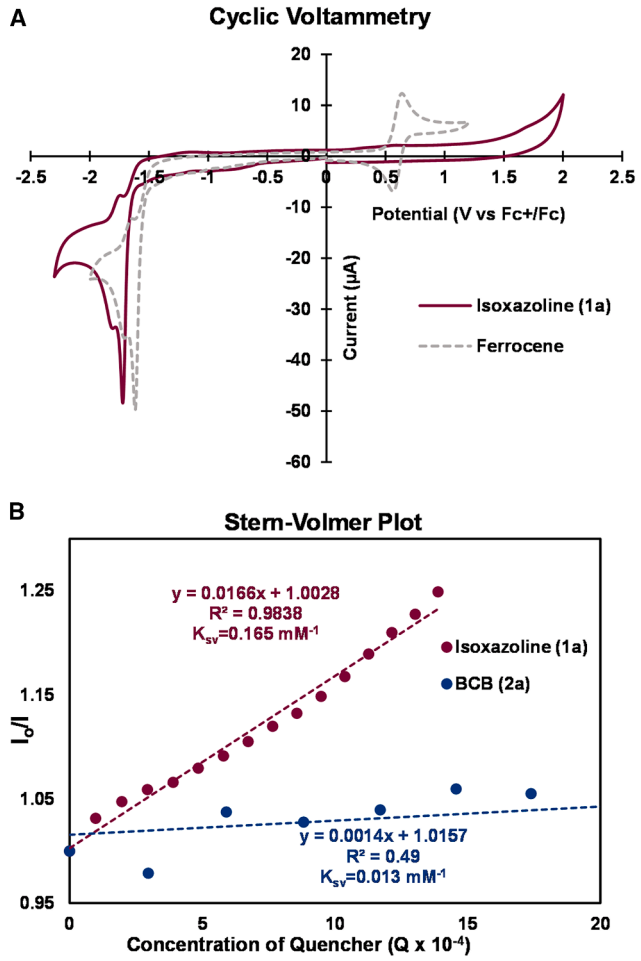

Figure 5. Mechanistic studies
(A) Cyclic voltammetry of **1a**.
(B) Stern-Volmer plot of **1a** and **2a**.

isoxazoline **1a**, sensitizing it to its triplet state ^{3}**1a***, which can form two exciplexes, **EC-1** (from *R*-isoxazoline **1a**) and **EC-2** (from *S*-isoxazoline **1a**), based on the orientation of the phenyl group (Figure 7). The reaction proceeds via attack of carbon C2 of isoxazoline on the terminal carbon C3 of BCB via **TS1** or **TS2** to generate a triplet biradical, which then undergoes ring closure by the MECP (minimum energy crossing point) to form the diastereomers **P1** and **P2**. The *trans*-isomer **P2** represents the thermodynamically more stable diastereomer and the major product, as confirmed by the 2D NMR spectrum. Additionally, the possibility of nitrogen N1 attack on C3 was also evaluated, but the activation barrier was found to be higher (see the supplemental methods for more details). The full energy profile is depicted in Figure 7. In the case of bisubstituted BCBs, the observed regioselectivity arises from preferential C-centered radical addition of the excited-state isoxazoline to the carbon atom bearing the electron-withdrawing group (EWG) on the BCBs. This preference is driven by the formation of a more stable benzylic radical intermediate, consistent with literature reports.[30,60]

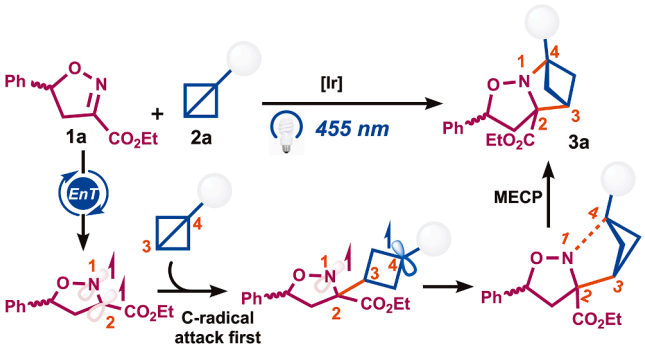

Figure 6. Plausible reaction mechanism
Proposed reaction mechanism via energy-transfer catalysis.

Synthetic utility

Given its relevance to medicinal chemistry, we pursued the synthesis of 5,5-disubstituted 2,4-methanoprolines. The general route to access such molecules relies on a linear synthetic strategy starting from allyl amines, followed by cycloaddition under UV irradiation.[24] Although bridged pyrrolidines bearing a single C5 substituent are commercially available, their demanding synthetic routes render large-scale procurement prohibitively expensive.[71]

Starting from selected cycloaddition products **3**, the N–O bond cleavage concurrent with the deoxygenation of the resulting benzyl alcohol readily occurred under palladium catalysis in an ambient hydrogen atmosphere, resulting in the exclusive formation of the products **4**, representing bridged proline derivatives (Figure 8). In the case of compound **3aq**, concurrent cleavage of both the benzylic C–N and C–O bonds was observed, furnishing a highly substituted, functionalized amino ester **5a** as the single diastereomer in an excellent yield. Other common late-stage modifications, including ester hydrolysis and reduction of cycloadduct **3aq**, furnished the corresponding products **5b** and **5c**.

In summary, this study demonstrates the efficient photocatalytic synthesis of isoxazolidine-fused bridged pyrrolidines. Considering that the isoxazoline precursors were in turn accessed via the copper(II) photoredox-catalyzed coupling between ethyl-2-nitroacetate and alkenes,[67] the overall two-step transformation integrates two well-established photochemical modes, i.e., SET and EnT that generate novel, highly complex scaffolds from readily available starting materials. The geometric parameters of compound **3i** were computed using DFT and benchmarked against its experimentally determined crystal structure. The same level of theory was applied to optimize the corresponding benzofuran analog bearing an identical substitution pattern for a direct comparison of exit vector orientations (Figure 9). The results demonstrate a close agreement between the calculated geometries and the steric parameters obtained from X-ray diffraction (XRD) analysis of the bridged bicyclic scaffold **3i**. These findings indicate that such frameworks may serve as promising isosteric replacements for medicinally relevant bicyclic heteroarenes.

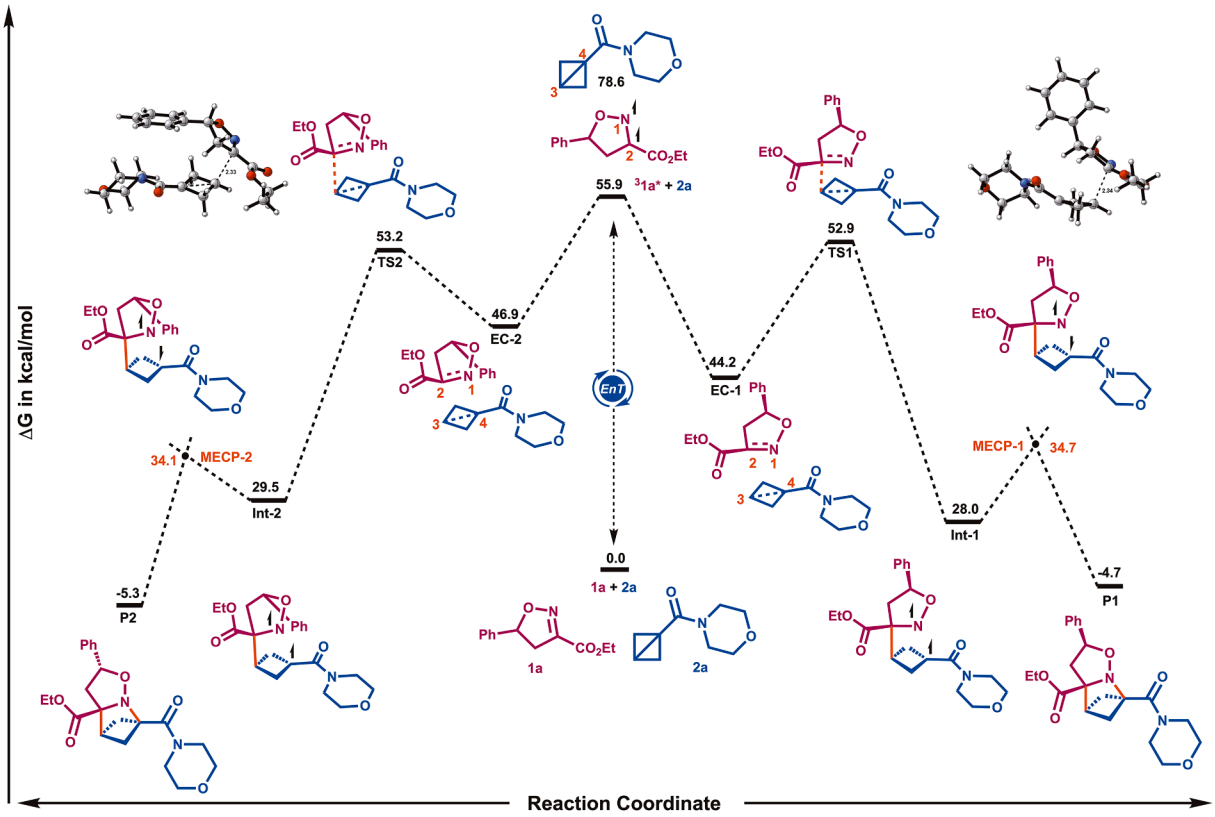

Figure 7. Reaction energy profile

Reaction profile for formation of both diastereomers calculated in (SMD: acetonitrile) B3LYP-D3BJ/def2-TZVP level of theory. All free energies are in kcal/mol. The energies of MECP were evaluated from the difference of electronic energies of the geometries at the crossing point and the triplet intermediates. The full details can be found in the supplemental methods.

METHODS

General procedure for the photochemical reaction between isoxazolines and BCBs

A 5 mL crimp-cap vial equipped with a Teflon-coated magnetic stirring bar was charged with the isoxazoline derivative **1** (0.10 mmol, 1.0 equiv), [Ir(dFppy)$_3$] (0.4 mg, 0.005 equiv, 0.5 mol %), and the bicyclobutane (BCB) derivative **2** (0.15 mmol, 1.5 equiv). The vial was sealed with a crimp cap, evacuated, and backfilled with nitrogen three times. Dry MeCN (1.0 mL) was then added under a positive nitrogen atmosphere. The reaction mixture was degassed by purging with nitrogen for 5 min and then irradiated with blue LEDs (λ_{max} = 455 nm, 6 W optical power). Upon completion (~20 h), the mixture was diluted with DCM (10 mL), transferred to a round-bottomed flask, and concentrated *in vacuo*. The crude residue was purified by flash column chromatography on a Büchi Pure C-815 flash system (eluent: DCM/EtOAc) to afford the desired products **3**.

General information

Commercially available chemicals were purchased in high quality and were used without further purification. Thereby, the weight was calculated based on the purity mentioned on the container. All reactions were carried out in oven-dried glassware under atmospheric conditions unless otherwise stated. Reactions with moisture- or oxygen-sensitive reagents were performed in flame-dried glassware under an atmosphere of predried nitrogen. All photochemical reactions were carried out at room temperature. Reactions were monitored by thin-layer chromatography (TLC) or crude ^{1}H-NMR analysis. Anhydrous solvents were prepared by established laboratory procedures or obtained from a solvent purification system (SPS). DCM, EtOAc, n-pentane, and hexanes (40°C–60°C) for chromatography were distilled prior to use. The reported yields are referred to isolated compounds unless otherwise stated.

Chromatography

Thin-layer chromatography (TLC) was performed with TLC precoated aluminum sheets (Merck; Silica gel 60 F254 [0.2-mm layer thickness]) and visualized by a dual-short (λ = 254 nm)/long (λ = 366 nm) wavelength UV lamp or stained with potassium permanganate solution. Column chromatography was performed with silica gel (Merck, 0.063–0.200-mm particle size) and flash silica gel (Merck, 0.040–0.063 mm particle size). Automated flash column chromatography was performed on a Büchi Pure C-815 flash system with an inbuilt UV and evaporative light scattering (ELS) detector.

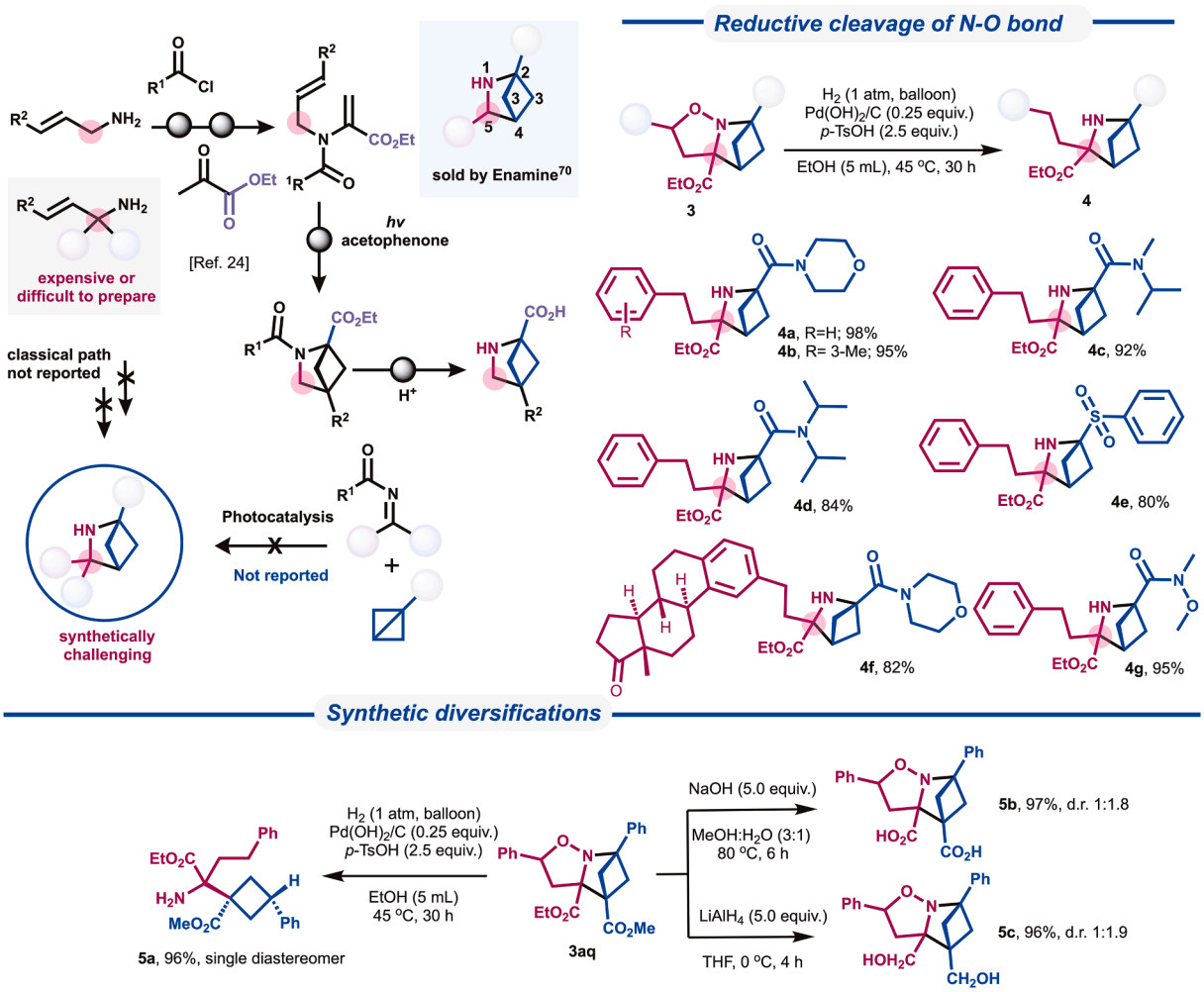

Figure 8. Synthetic utility of products
Synthetic utility of cycloadduct **3**.

NMR spectroscopy

^{1}H-NMR spectra were recorded on a Bruker Avance 300 (300 MHz), Bruker Avance 400 (400 MHz), or Bruker Avance III 400 "Nanobay" (400 MHz) spectrometer. Chemical shifts (δ [ppm]) are reported in parts per million (ppm) and referenced to CDCl3 (^{1}H: 7.26 ppm; ^{13}C: 77.16 ppm). Coupling constants

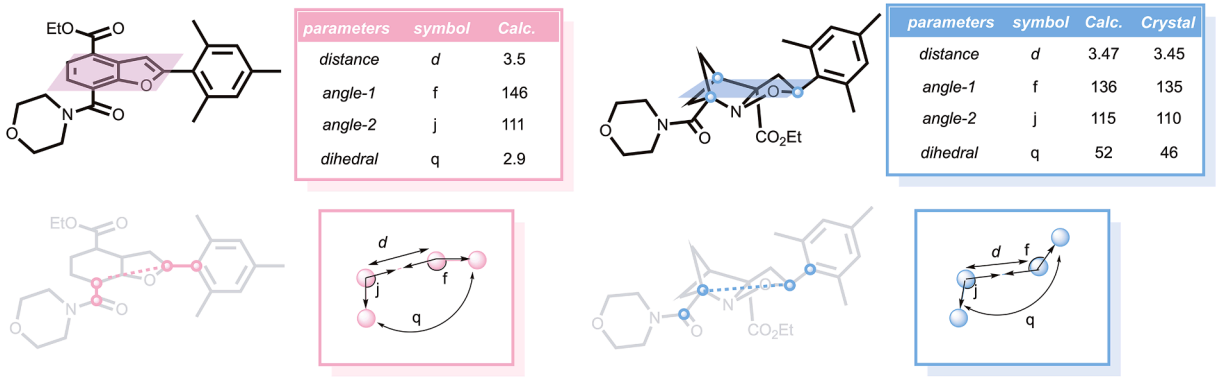

Figure 9. Exit vector analysis
Exit vector analysis: comparison of product **3i** with the related benzofuran derivative. All the structures are calculated at the B3LYP-D3BJ/def2-TZVP level of theory.

(J) are given in Hertz (Hz) and refer to corresponding multiplicities (s = singlet, d = doublet, t = triplet, q = quartet, quin = quintet, hex = hextet, h = heptet, m = multiplet, dd = doublet of doublets, br. = broad signal, etc.). The ^{1}H-NMR spectra are reported as follows: chemical shift (multiplicity, coupling constants, and number of protons). NMR assignments were made according to spin systems, using 2D NMR spectroscopy (COSY, HSQC, and HMBC) to assist with characterization. NMR yields were determined by ^{1}H-NMR analysis using 1,1,2,2-tetrachlorethane as an internal standard.

^{19}F-NMR spectra were recorded on a Bruker Avance 300 (282 MHz), Bruker Avance 400 (376 MHz), or Bruker Avance III 400 "Nanobay" (376 MHz) spectrometer.

Mass spectrometry

Mass spectra were recorded by the Central Analytic Department of the University of Regensburg using JEOL AccuTOF GCX and an Agilent Q-TOF 6540 UHD spectrometer. High-resolution mass spectra were measured using atmospheric pressure chemical ionization (APCI), electron ionization (EI), or electrospray ionization (ESI) with a quadrupole time-of-flight (Q-TOF) detector.

X-ray crystallography

X-ray crystallographic analysis was performed by the Central Analytic Department of the University of Regensburg using an Agilent Technologies SuperNova, an Agilent Technologies Gemini R Ultra, an Agilent GV 50, or a Rigaku GV 50 diffractometer. Suitable crystals were mounted on a Lindemann tube oil and kept at a steady temperature of T = 293 K during data collection. The structures were solved with the ShelXT structure solution program using the Intrinsic Phasing solution method and Olex2 as the graphical interface. The model was refined with ShelXL using least-square minimization.

RESOURCE AVAILABILITY

Lead contact

Requests for further information, resources, and reagents should be directed to and will be fulfilled by the lead contact, Oliver Reiser (oliver.reiser@chemie.uni-regensburg.de).

Materials availability

All chemical materials and experimental procedures are summarized in the text and in the supplemental methods.

Data and code availability

- All data related to the findings of this article are included in the main text or in the supplemental methods.
- Any additional information required to reanalyze the data reported in this paper is available from the lead contact upon request.
- The primary research data underlying this study are openly available in Radar4Chem at doi:10.22000/d030q1jdkufq68q0
- X-ray data have been deposited in the CCDC under reference numbers CCDC: 2550266 (**3f**) and 2518812 (**3i**).

ACKNOWLEDGMENTS

This work was supported by the German Academic Exchange (DAAD, fellowship for S.S.) and the Deutsche Forschungsgemeinschaft (TRR 325444632635-A2). We thank Regina Hoheisel for performing the cyclic voltammetry measurements; Sabine Stempfhuber and Birgit Hischa for X-ray analysis; and Dr. Aryaman Pattanaik, Arezoo Tanbakoochian, and Prithwa Das for scientific discussions (all University of Regensburg). We thank Hina Shahzadi (SynCat, University of Regensburg) for the synthesis of isoxazoline starting materials as part of her practical course in the Master's curriculum. We are also thankful to Central Mass and NMR Facilities at the University of Regensburg.

AUTHOR CONTRIBUTIONS

S.S. and O.R. conceived the project; S.S. carried out all synthetic experiments, data analysis, and DFT calculations; and O.R. and S.S. wrote the manuscript.

DECLARATION OF INTERESTS

The authors declare no conflicts of interest.

SUPPLEMENTAL INFORMATION

Supplemental information can be found online at https://doi.org/10.1016/j.xcrp.2026.103449.

Received: January 22, 2026
Revised: May 5, 2026
Accepted: June 30, 2026

REFERENCES

1. Polêto, M.D., Rusu, V.H., Grisci, B.I., Dorn, M., Lins, R.D., and Verli, H. (2018). Aromatic Rings Commonly Used in Medicinal Chemistry: Force Fields Comparison and Interactions With Water Toward the Design of New Chemical Entities. Front. Pharmacol. *9*, 395. https://doi.org/10.3389/fphar.2018.00395.
2. Subbaiah, M.A.M., and Meanwell, N.A. (2021). Bioisosteres of the Phenyl Ring: Recent Strategic Applications in Lead Optimization and Drug Design. J. Med. Chem. *64*, 14046–14128. https://doi.org/10.1021/acs.jmedchem.1c01215.
3. Zhang, M., Chapman, M., Sarode, B.R., Xiong, B., Liang, H., Chen, J.K., Weerapana, E., and Morken, J.P. (2024). Catalytic asymmetric synthesis of meta benzene isosteres. Nature *633*, 90–95. https://doi.org/10.1038/s41586-024-07865-4.
4. Keri, R.S., Chand, K., Budagumpi, S., Balappa Somappa, S., Patil, S.A., and Nagaraja, B.M. (2017). An overview of benzo [b] thiophene-based medicinal chemistry. Eur. J. Med. Chem. *138*, 1002–1033. https://doi.org/10.1016/j.ejmech.2017.07.038.
5. Radadiya, A., and Shah, A. (2015). Bioactive benzofuran derivatives: An insight on lead developments, radioligands and advances of the last decade. Eur. J. Med. Chem. *97*, 356–376. https://doi.org/10.1016/j.ejmech.2015.01.021.
6. Zeng, W., Han, C., Mohammed, S., Li, S., Song, Y., Sun, F., and Du, Y. (2024). Indole-containing pharmaceuticals: targets, pharmacological activities, and SAR studies. RSC Med. Chem. *15*, 788–808. https://doi.org/10.1039/d3md00677h.
7. Denisenko, A., Garbuz, P., Shishkina, S.V., Voloshchuk, N.M., and Mykhailiuk, P.K. (2020). Saturated Bioisosteres of ortho-Substituted Benzenes. Angew. Chem. Int. Ed. *59*, 20515–20521. https://doi.org/10.1002/anie.202004183.
8. Herter, L., Koutsopetras, I., Turelli, L., Fessard, T., and Salomé, C. (2022). Preparation of new bicyclo2.1.1hexane compact modules: an opening towards novel sp3-rich chemical space. Org. Biomol. Chem. *20*, 9108–9111. https://doi.org/10.1039/d2ob01669a.
9. Rigotti, T., and Bach, T. (2022). Bicyclo2.1.1hexanes by Visible Light-Driven Intramolecular Crossed 2 + 2 Photocycloadditions. Org. Lett. *24*, 8821–8825. https://doi.org/10.1021/acs.orglett.2c03606.

10. Mykhailiuk, P.K. (2019). Saturated bioisosteres of benzene: where to go next? Org. Biomol. Chem. *17*, 2839–2849. https://doi.org/10.1039/c8ob02812e.

11. Ritchie, T.J., and Macdonald, S.J.F. (2009). The impact of aromatic ring count on compound developability–are too many aromatic rings a liability in drug design? Drug Discov. Today *14*, 1011–1020. https://doi.org/10.1016/j.drudis.2009.07.014.

12. Cox, B., Zdorichenko, V., Cox, P.B., Booker-Milburn, K.I., Paumier, R., Elliott, L.D., Robertson-Ralph, M., and Bloomfield, G. (2020). Escaping from Flatland: Substituted Bridged Pyrrolidine Fragments with Inherent Three-Dimensional Character. ACS Med. Chem. Lett. *11*, 1185–1190. https://doi.org/10.1021/acsmedchemlett.0c00039.

13. Lovering, F. (2013). Escape from Flatland 2: complexity and promiscuity. Med. Chem. Commun. *4*, 515. https://doi.org/10.1039/c2md20347b.

14. Lovering, F., Bikker, J., and Humblet, C. (2009). Escape from flatland: increasing saturation as an approach to improving clinical success. J. Med. Chem. *52*, 6752–6756. https://doi.org/10.1021/jm901241e.

15. Almehmadi, Y.A., McGeehan, J., Guzman, N.J., Christensen, K.E., Yamazaki, K., and Dixon, D.J. (2024). Iridium-catalysed synthesis of C,N,N-cyclic azomethine imines enables entry to unexplored nitrogen-rich 3D chemical space. Nat. Synth. *3*, 1168–1175. https://doi.org/10.1038/s44160-024-00574-w.

16. Levterov, V.V., Panasiuk, Y., Sahun, K., Stashkevych, O., Badlo, V., Shablykin, O., Sadkova, I., Bortnichuk, L., Klymenko-Ulianov, O., Holota, Y., et al. (2023). 2-Oxabicyclo[2.2.2]octane as a new bioisostere of the phenyl ring. Nat. Commun. *14*, 5608. https://doi.org/10.1038/s41467-023-41298-3.

17. Ma, J., Chen, S., Bellotti, P., Wagener, T., Daniliuc, C., Houk, K.N., and Glorius, F. (2022). Facile access to fused 2D/3D rings via intermolecular cascade dearomative [2 + 2] cycloaddition/rearrangement reactions of quinolines with alkenes. Nat. Catal. *5*, 405–413. https://doi.org/10.1038/s41929-022-00784-5.

18. Roland, G., Hurdal, K.N., Bouchouicha, A., Dowe, N., Davis, R.L., and Collins, S.K. (2024). [2 + 2] Photocycloadditions to Form Cyclobutanes and Bicyclo[2.1.1]hexanes Employing Copper-Based Photocatalysis. ACS Catal. *14*, 11490–11497. https://doi.org/10.1021/acscatal.4c03218.

19. Dibchak, D., Snisarenko, M., Mishuk, A., Shablykin, O., Bortnichuk, L., Klymenko-Ulianov, O., Kheylik, Y., Sadkova, I.V., Rzepa, H.S., and Mykhailiuk, P.K. (2023). General Synthesis of 3-Azabicyclo3.1.1heptanes and Evaluation of Their Properties as Saturated Isosteres. Angew. Chem. Int *62*, e202304246. https://doi.org/10.1002/anie.202304246.

20. Li Petri, G., Raimondi, M.V., Spanò, V., Holl, R., Barraja, P., and Montalbano, A. (2021). Pyrrolidine in Drug Discovery: A Versatile Scaffold for Novel Biologically Active Compounds. Top. Curr. Chem. *379*, 34. https://doi.org/10.1007/s41061-021-00347-5.

21. Poyraz, S., Döndaş, H.A., Döndaş, N.Y., and Sansano, J.M. (2023). Recent insights about pyrrolidine core skeletons in pharmacology. Front. Pharmacol. *14*, 1239658. https://doi.org/10.3389/fphar.2023.1239658.

22. Sahu, R., Shah, K., Malviya, R., Paliwal, D., Sagar, S., Singh, S., and Prajapati, B.G. (2024). Recent advancement in pyrrolidine moiety for the management of cancer: A review. Results Chem. *7*, 101301. https://doi.org/10.1016/j.rechem.2023.101301.

23. Ye, D., Lu, H., He, Y., Zheng, Z., Wu, J., and Wei, H. (2022). Rapid syntheses of N-fused heterocycles via acyl-transfer in heteroaryl ketones. Nat. Commun. *13*, 3337. https://doi.org/10.1038/s41467-022-31063-3.

24. Levterov, V.V., Michurin, O., Borysko, P.O., Zozulya, S., Sadkova, I.V., Tolmachev, A.A., and Mykhailiuk, P.K. (2018). Photochemical In-Flow Synthesis of 2,4-Methanopyrrolidines: Pyrrolidine Analogues with Improved Water Solubility and Reduced Lipophilicity. J. Org. Chem. *83*, 14350–14361. https://doi.org/10.1021/acs.joc.8b02071.

25. Savych, V.I., Mykhalchuk, V.L., Melnychuk, P.V., Isakov, A.O., Savchuk, T., Timoshenko, V.M., Siry, S.A., Pavlenko, S.O., Kovalenko, D.V., Hryshchuk, O.V., et al. (2021). Bicyclic Pyrrolidines for Medicinal Chemistry via 3 + 2-Cycloaddition. J. Org. Chem. *86*, 13289–13309. https://doi.org/10.1021/acs.joc.1c01327.

26. Yu, I.F., Manske, J.L., Diéguez-Vázquez, A., Misale, A., Pashenko, A.E., Mykhailiuk, P.K., Ryabukhin, S.V., Volochnyuk, D.M., and Hartwig, J.F. (2023). Catalytic undirected borylation of tertiary C-H bonds in bicyclo1.1.1pentanes and bicyclo2.1.1hexanes. Nat. Chem. *15*, 685–693. https://doi.org/10.1038/s41557-023-01159-4.

27. Agasti, S., Beltran, F., Pye, E., Kaltsoyannis, N., Crisenza, G.E.M., and Procter, D.J. (2023). A catalytic alkene insertion approach to bicyclo2.1.1-hexane bioisosteres. Nat. Chem. *15*, 535–541. https://doi.org/10.1038/s41557-023-01135-y.

28. Denisenko, A., Garbuz, P., Voloshchuk, N.M., Holota, Y., Al-Maali, G., Borysko, P., and Mykhailiuk, P.K. (2023). 2-Oxabicyclo2.1.1hexanes as saturated bioisosteres of the ortho-substituted phenyl ring. Nat. Chem. *15*, 1155–1163. https://doi.org/10.1038/s41557-023-01222-0.

29. Dutta, S., Lee, D., Ozols, K., Daniliuc, C.G., Shintani, R., and Glorius, F. (2024). Photoredox-Enabled Dearomative 2π + 2σ Cycloaddition of Phenols. J. Am. Chem. Soc. *146*, 2789–2797. https://doi.org/10.1021/jacs.3c12894.

30. Chintawar, C.C., Laskar, R., Rana, D., Schäfer, F., Schäfer, F., Dutta, S., Daniliuc, C.G., and Glorius, F. (2024). Photoredox-Catalyzed Amidyl Radical Insertion to Bicyclo[1.1.0]butanes. Nat. Catal. *7*, 1232–1242. https://doi.org/10.1038/s41929-024-01239-9.

31. Guo, R., Chang, Y.-C., Herter, L., Salome, C., Braley, S.E., Fessard, T.C., and Brown, M.K. (2022). Strain-Release 2π + 2σ Cycloadditions for the Synthesis of Bicyclo2.1.1hexanes Initiated by Energy Transfer. J. Am. Chem. Soc. *144*, 7988–7994. https://doi.org/10.1021/jacs.2c02976.

32. Hu, S., Pan, Y., Ni, D., and Deng, L. (2024). Facile access to bicyclo2.1.1-hexanes by Lewis acid-catalyzed formal cycloaddition between silyl enol ethers and bicyclo1.1.0butanes. Nat. Commun. *15*, 6128. https://doi.org/10.1038/s41467-024-50434-6.

33. Kleinmans, R., Dutta, S., Ozols, K., Shao, H., Schäfer, F., Thielemann, R.E., Chan, H.T., Daniliuc, C.G., Houk, K.N., and Glorius, F. (2023). ortho-Selective Dearomative 2π + 2σ Photocycloadditions of Bicyclic Aza-Arenes. J. Am. Chem. Soc. *145*, 12324–12332. https://doi.org/10.1021/jacs.3c02961.

34. Kleinmans, R., Pinkert, T., Dutta, S., Paulisch, T.O., Keum, H., Daniliuc, C.G., and Glorius, F. (2022). Intermolecular 2π+2σ-photocycloaddition enabled by triplet energy transfer. Nature *605*, 477–482. https://doi.org/10.1038/s41586-022-04636-x.

35. Li, Y.-J., Wu, Z.-L., Gu, Q.-S., Fan, T., Duan, M.-H., Wu, L., Wang, Y.-T., Wu, J.-P., Fu, F.-L., Sang, F., et al. (2024). Catalytic Intermolecular Asymmetric 2π + 2σ Cycloadditions of Bicyclo1.1.0butanes: Practical Synthesis of Enantioenriched Highly Substituted Bicyclo2.1.1hexanes. J. Am. Chem. Soc. *146*, 34427–34441. https://doi.org/10.1021/jacs.4c10968.

36. Ma, J., Chen, S., Bellotti, P., Guo, R., Schäfer, F., Heusler, A., Zhang, X., Daniliuc, C., Brown, M.K., Houk, K.N., and Glorius, F. (2021). Photochemical intermolecular dearomative cycloaddition of bicyclic azaarenes with alkenes. Science *371*, 1338–1345. https://doi.org/10.1126/science.abg0720.

37. Robichon, M. de, Kratz, T., Beyer, F., Zuber, J., Merten, C., and Bach, T. (2023). Enantioselective, Intermolecular π2+σ2 Photocycloaddition Reactions of 2(1H)-Quinolones and Bicyclo1.1.0butanes. J. Am. Chem. Soc. *145*, 24466–24470.

38. Singha, T., Bapat, N.A., Mishra, S.K., and Hari, D.P. (2024). Photoredox-Catalyzed Strain-Release-Driven Synthesis of Functionalized Spirocyclobutyl Oxindoles. Org. Lett. *26*, 6396–6401. https://doi.org/10.1021/acs.orglett.4c02177.

39. Su, J.-Y., Zhang, J., Xin, Z.-Y., Zheng, H., Li, H., and Deng, W.-P. (2024). Access to Spiro-bicyclo[2.1.1]hexanes via BF3·Et2O-Catalyzed Formal [2π + 2σ] Cycloaddition of Bicyclo[1.1.0]butanes with Benzofuran-derived Oxa(aza)dienes.Org. Chem. Front. *11*, 4539–4545.

40. Tian, S., Liu, R., Zhang, K., Xia, Y., Liu, Y., Li, P., Duan, X.-H., and Guo, L.-N. (2025). Substrate-Regulated Divergent Addition of N-Sulfonyl Ketimines to Bicyclo1.1.0butanes Enabled by Photoinduced Energy Transfer. Org. Lett. *27*, 3818–3824. https://doi.org/10.1021/acs.orglett.5c00189.

41. Wang, H., Shao, H., Das, A., Dutta, S., Chan, H.T., Daniliuc, C., Houk, K.N., and Glorius, F. (2023). Dearomative ring expansion of thiophenes by bicyclobutane insertion. Science *381*, 75–81. https://doi.org/10.1126/science.adh9737.

42. Liu, Y., Lin, S., Li, Y., Xue, J.-H., Li, Q., and Wang, H. (2023). Pyridine-Boryl Radical-Catalyzed [2π + 2σ] Cycloaddition of Bicyclo[1.1.0]butanes with Alkenes. ACS Catal. *13*, 5096–5103. https://doi.org/10.1021/acscatal.3c00305.

43. Xu, M., Wang, Z., Sun, Z., Ouyang, Y., Ding, Z., Yu, T., Xu, L., and Li, P. (2022). Diboron(4)-Catalyzed Remote 3+2 Cycloaddition of Cyclopropanes via Dearomative/Rearomative Radical Transmission through Pyridine. Angew. Chem. Int. Ed. *61*, e202214507. https://doi.org/10.1002/anie.202214507.

44. Nicolai, S., and Waser, J. (2024). Lewis acid catalyzed 4+2 annulation of bicyclobutanes with dienol ethers for the synthesis of bicyclo4.1.1octanes. Chem. Sci. *15*, 10823–10829. https://doi.org/10.1039/d4sc02767a.

45. Chang, Y.-C., Salome, C., Fessard, T., and Brown, M.K. (2023). Synthesis of 2-Azanorbornanes via Strain-Release Formal Cycloadditions Initiated by Energy Transfer. Angew. Chem. Int. Ed. *62*, e202314700. https://doi.org/10.1002/anie.202314700.

46. Yang, J., Yao, B.-X., Jiang, H.-F., Ni, S.-F., Dixneuf, P.H., and Zhang, M. (2025). Direct Access to Functional 2-Azabicyclo2.1.1Hexanes via Hydrodearomative 2π + 2σ Cycloaddition of Aza-Arenes. Angew. Chem. Int. Ed. *64*, e202505060. https://doi.org/10.1002/anie.202505060.

47. Chang, Y.-C., Martín, M., Bortey, K., Lefebvre, Q., Fessard, T., Salome, C., Vázquez, R.J., and Brown, M.K. (2025). Catalyst-Controlled Regiodivergent Synthesis of Bicyclo2.1.1hexanes via Photochemical Strain-Release Cycloadditions. J. Am. Chem. Soc. *147*, 14936–14944. https://doi.org/10.1021/jacs.5c02425.

48. Golfmann, M., Reinhold, M., Steen, J.D., Deike, M.S., Rodemann, B., Golz, C., Crespi, S., and Walker, J.C.L. (2024). Photocatalytic Oxidative Activation of Bicyclo[1.1.0]butanes for Formal [2σ+2π] Cycloadditions. ACS Catal. *14*, 13987–13998. https://doi.org/10.1021/acscatal.4c05067.

49. Li, Y., Gu, X., Wei, Y., and Shi, M. (2025). Intramolecular dearomative [2π + 2σ] photocycloadditions of bicyclo[1.1.0]butanes with (benzo)furans and (benzo)thiophenes initiated by energy transfer or single electron transfer. Sci. China Chem. *68*, 4959–4972. https://doi.org/10.1007/s11426-025-2704-x.

50. Hu, Q.-Q., Chen, J., Yang, Y., Yang, H., and Zhou, L. (2024). Strain-release transformations of bicyclo[1.1.0]butanes and [1.1.1]propellanes. Tetrahedron Chem *9*, 100070. https://doi.org/10.1016/j.tchem.2024.100070.

51. Radhoff, N., Daniliuc, C.G., and Studer, A. (2023). Lewis Acid Catalyzed Formal (3+2)-Cycloaddition of Bicyclo1.1.0butanes with Ketenes. Angew. Chem. Int. Ed. *62*, e202304771. https://doi.org/10.1002/anie.202304771.

52. Liang, Y., Paulus, F., Daniliuc, C.G., and Glorius, F. (2023). Catalytic Formal 2π+2σ Cycloaddition of Aldehydes with Bicyclobutanes: Expedient Access to Polysubstituted 2-Oxabicyclo2.1.1hexanes. Angew. Chem. Int. Ed. *62*, e202305043. https://doi.org/10.1002/anie.202305043.

53. Hu, Q.-Q., Wang, L.-Y., Chen, X.-H., Geng, Z.-X., Chen, J., and Zhou, L. (2024). Lewis Acid Catalyzed Cycloaddition of Bicyclobutanes with Ynamides for the Synthesis of Polysubstituted 2-Amino-bicyclo2.1.1hexenes. Angew. Chem. Int. Ed. *63*, e202405781. https://doi.org/10.1002/anie.202405781.

54. Yang, L., Wang, H., Lang, M., Wang, J., and Peng, S. (2024). B(C6F5)3-Catalyzed Formal (n + 3) (n = 5 and 6) Cycloaddition of Bicyclo1.1.0butanes to Medium Bicyclon.1.1alkanes. Org. Lett. *26*, 4104–4110. https://doi.org/10.1021/acs.orglett.4c01219.

55. Ni, D., Hu, S., Tan, X., Yu, Y., Li, Z., and Deng, L. (2023). Intermolecular Formal Cycloaddition of Indoles with Bicyclo1.1.0butanes by Lewis Acid Catalysis. Angew. Chem. Int. Ed. *62*, e202308606. https://doi.org/10.1002/anie.202308606.

56. Tang, L., Xiao, Y., Wu, F., Zhou, J.-L., Xu, T.-T., and Feng, J.-J. (2023). Silver-Catalyzed Dearomative 2π+2σ Cycloadditions of Indoles with Bicyclobutanes: Access to Indoline Fused Bicyclo2.1.1hexanes. Angew. Chem. Int. Ed. *62*, e202310066. https://doi.org/10.1002/anie.202310066.

57. Dhake, K., Woelk, K.J., Becica, J., Un, A., Jenny, S.E., and Leitch, D.C. (2022). Beyond Bioisosteres: Divergent Synthesis of Azabicyclohexanes and Cyclobutenyl Amines from Bicyclobutanes. Angew. Chem. Int. Ed. *61*, e202204719. https://doi.org/10.1002/anie.202204719.

58. Zhang, X.-G., Chen, J.-J., Zhou, Z.-Y., Li, J.-X., and Zhou, Q.-L. (2025). Enantioselective [2π + 2σ] cycloaddition of bicyclobutanes with imines: An efficient approach to chiral 2-aza-bicyclo[2.1.1]hexanes. Chem Catal. *5*, 101295. https://doi.org/10.1016/j.checat.2025.101295.

59. Wu, F., Wu, W.-B., Xiao, Y., Li, Z., Tang, L., He, H.-X., Yang, X.-C., Wang, J.-J., Cai, Y., Xu, T.-T., et al. (2024). Zinc-Catalyzed Enantioselective Formal (3+2) Cycloadditions of Bicyclobutanes with Imines: Catalytic Asymmetric Synthesis of Azabicyclo2.1.1hexanes. Angew. Chem. Int. Ed. *63*, e202406548. https://doi.org/10.1002/anie.202406548.

60. Yan, M., Ye, Z., and Lu, P. (2025). Catalyst-free, visible-light-induced [2π + 2σ] cycloaddition towards azabicyclohexanes. Chin. Chem. Lett. *36*, 110540. https://doi.org/10.1016/j.cclet.2024.110540.

61. Zhang, K., Tian, S., Li, W., Yang, X., Duan, X.-H., Guo, L.-N., and Li, P. (2024). Lewis Acid-Catalyzed Formal 2π+2σ Cycloaddition of Bicyclobutanes with Quinoxalin-2(1H)-ones: Access to Quinoxaline-Fused Aza-Bicyclo2.1.1hexanes. Org. Lett. *26*, 5482–5487. https://doi.org/10.1021/acs.orglett.4c01775.

62. Amărandi, R.-M., Al-Matarneh, M.-C., Popovici, L., Ciobanu, C.I., Neamțu, A., Mangalagiu, I.I., and Danac, R. (2023). Exploring Pyrrolo-Fused Heterocycles as Promising Anticancer Agents: An Integrated Synthetic, Biological, and Computational Approach. Pharmaceuticals *16*, 865. https://doi.org/10.3390/ph16060865.

63. Heravi, M.M., and Zadsirjan, V. (2020). Prescribed drugs containing nitrogen heterocycles: an overview. RSC Adv. *10*, 44247–44311. https://doi.org/10.1039/d0ra09198g.

64. Ouzounthanasis, K.A., Rizos, S.R., and Koumbis, A.E. (2023). A Convenient Synthesis of Novel Isoxazolidine and Isoxazole Isoquinolinones Fused Hybrids. Molecules *29*, 91. https://doi.org/10.3390/molecules29010091.

65. Pibiri, I. (2024). Recent Advances: Heterocycles in Drugs and Drug Discovery. Int. J. Mol. Sci. *25*, 9503. https://doi.org/10.3390/ijms25179503.

66. Rusu, A., Moga, I.-M., Uncu, L., and Hancu, G. (2023). The Role of Five-Membered Heterocycles in the Molecular Structure of Antibacterial Drugs Used in Therapy. Pharmaceutics *15*, 2554. https://doi.org/10.3390/pharmaceutics15112554.

67. Sardana, S., Pattanaik, A., Rehbein, J., and Reiser, O. (2025). Copper(II)-Photocatalyzed Radical Anellation of Nitroalkanes with Alkenes or Alkynes for the Synthesis of Isoxazolines and Isoxazoles. Angew. Chem. Int. Ed. *64*, e202509658. https://doi.org/10.1002/anie.202509658.

68. Huang, J., Zhou, T.-P., Sun, N., Yu, H., Yu, X., Liao, R.-Z., Yao, W., Dai, Z., Wu, G., and Zhong, F. (2024). Accessing ladder-shape azetidine-fused indoline pentacycles through intermolecular regiodivergent aza-Paternò-Büchi reactions. Nat. Commun. *15*, 1431. https://doi.org/10.1038/s41467-024-45687-0.

69. Day, J.I., Teegardin, K., Weaver, J., and Chan, J. (2016). Advances in Photocatalysis: A Microreview of Visible Light Mediated Ruthenium and Iridium Catalyzed Organic Transformations. Org. Process Res. Dev. *20*, 1156–1163. https://doi.org/10.1021/acs.oprd.6b00101.

70. Becker, M.R., Wearing, E.R., and Schindler, C.S. (2020). Synthesis of azetidines via visible-light-mediated intermolecular 2+2 photocycloadditions. Nat. Chem. *12*, 898–905. https://doi.org/10.1038/s41557-020-0541-1.

71. Enamine. https://enamine.net/building-blocks/medchem/bridged-pyrrolidine-with-reduced-lipophilicity?highlight=WyJicmlkZ2VkIl0=.